AFRL-RV-PS-
TP-2012-0038

AFRL-RV-PS-
TP-2012-0038

CRUST AND UPPER MANTLE STRUCTURE FROM JOINT INVERSION OF BODY WAVE AND GRAVITY DATA (POSTPRINT)

Annual Report 1

Eric A. Bergman, et al.

University of Colorado
3100 Marine Street
Boulder, CO 80303-1058

10 May 2012

Technical Paper

APPROVED FOR PUBLIC RELEASE; DISTRIBUTION IS UNLIMITED.

AIR FORCE RESEARCH LABORATORY
Space Vehicles Directorate
3550 Aberdeen Ave SE
AIR FORCE MATERIEL COMMAND
KIRTLAND AIR FORCE BASE, NM 87117-5776

REPORT DOCUMENTATION PAGE

Form Approved
OMB No. 0704-0188

1. REPORT DATE
10 May 2012

2. REPORT TYPE
Technical Paper

3. DATES COVERED *(From - To)*
01 Sep 2010 to 19 Mar 2012

4. TITLE AND SUBTITLE
Crust and Upper Mantle Structure from Joint Inversion of Body Wave and Gravity Data (POSTPRINT): Annual Report 1

5a. CONTRACT NUMBER
FA9453-11-1-0233

5b. GRANT NUMBER

5c. PROGRAM ELEMENT NUMBER
62601F

5d. PROJECT NUMBER
1010

5e. TASK NUMBER
PPM00009379

5f. WORK UNIT NUMBER
EF004136

6. AUTHOR(S)
Eric A. Bergman, Charlotte A. Rowe*, and Monica Maceira*

7. PERFORMING ORGANIZATION NAME(S) AND ADDRESS(ES)

University of Colorado
3100 Marine Street
Boulder, CO 80303-1058

8. PERFORMING ORGANIZATION REPORT NUMBER

9. SPONSORING / MONITORING AGENCY NAME(S) AND ADDRESS(ES)
Air Force Research Laboratory
Space Vehicles Directorate
3550 Aberdeen Ave SE
Kirtland AFB, NM 87117-5776

10. SPONSOR/MONITOR'S ACRONYM(S)
AFRL/RVBYE

11. SPONSOR/MONITOR'S REPORT NUMBER(S)
AFRL-RV-PS-TP-2012-0038

12. DISTRIBUTION / AVAILABILITY STATEMENT

Approved for public release; distribution is unlimited. (LA-UR-11-04823).

13. SUPPLEMENTARY NOTES
Published in The Proceedings of the 2011 Monitoring Research Review – Ground-Based Nuclear Explosion Monitoring Technologies, 13 – 15 September 2011, Tucson, AZ, Volume I, pp 30-38. Government Purpose Rights.

*Los Alamos National Laboratory

14. ABSTRACT

The crustal and upper mantle velocity structure of the region expressing the continental collision between the Arabian and Eurasian plates is being investigated using a joint inversion of body wave arrival times and satellite gravity. The body wave data set is derived from previous and on-going work on location calibration and includes a large (~1700 events) subset of events that qualify as GT590. The associated arrival time data sets for these events include many readings of direct crustal P and S phases, as well as regional (Pn and Sn) and teleseismic phases. The data set has been carefully groomed to identify and remove outlier readings and empirical reading errors are estimated for most arrivals from a multiple event relocation analysis. The gravity data provides valuable supplemental information on the lateral distribution of velocity variations that helps to compensate for incomplete raypath coverage in the body waveform data set, especially when bandpass filtering is used to constrain the gravity signal to depth ranges that are consistent with the body wave data. Experiments with smaller, higher-quality GT data sets as well as full data sets that include all available arrival time data in the region will be carried out to determine if the increase in precision and accuracy of GT-derived data adequately compensates for reduced numbers of data and raypaths.

15. SUBJECT TERMS
Seismic velocity models, Travel time tomography, Gravity, Joint inversion

16. SECURITY CLASSIFICATION OF: a. REPORT	b. ABSTRACT	c. THIS PAGE	17. LIMITATION OF ABSTRACT	18. NUMBER OF PAGES	19a. NAME OF RESPONSIBLE PERSON
Unclassified	Unclassified	Unclassified	Unlimited	12	Robert J. Raistrick
					19b. TELEPHONE NUMBER *(include area code)*

Standard Form 298 (Rev. 8-98)
Prescribed by ANSI Std. 239.18

CRUST AND UPPER MANTLE STRUCTURE FROM JOINT INVERSION OF BODY WAVE AND GRAVITY DATA

Eric A. Bergman[1], Charlotte A. Rowe[2], and Monica Maceira[2]

University of Colorado[1] and Los Alamos National Laboratory[2]

Sponsored by the Air Force Research Laboratory[1] and the National Nuclear Security Administration[2]

Award Nos. FA9453-11-1-0233[1] and LA11-BAA11-46-NDD03[2]
Proposal No. BAA11-46

ABSTRACT

We are investigating the crustal and upper mantle velocity structure of the region expressing the continental collision between the Arabian and Eurasian plates using a joint inversion of body wave arrival times and satellite gravity. The body wave data set is derived from previous and on-going work on location calibration and includes a large (~1700 events) subset of events that qualify as $GT5_{90}$. The associated arrival time data sets for these events include many readings of direct crustal P and S phases, as well as regional (Pn and Sn) and teleseismic phases. The data set has been carefully groomed to identify and remove outlier readings and empirical reading errors are estimated for most arrivals from a multiple event relocation analysis. The gravity data provides valuable supplemental information on the lateral distribution of velocity variations that helps to compensate for incomplete raypath coverage in the body waveform data set, especially when bandpass filtering is used to constrain the gravity signal to depth ranges that are consistent with the body wave data. We will carry out experiments with smaller, higher-quality GT data sets as well as full data sets that include all available arrival time data in the region, and try to determine if the increase in precision and accuracy of GT-derived data adequately compensates for reduced numbers of data and raypaths. We will compare our results on lateral heterogeneity of the crust and upper mantle velocities in this region with other studies and offer our results for integration into Lab-based research efforts to construct improved 3-D velocity models to support monitoring efforts in the region.

OBJECTIVES

Our objective in this project is to gain increased understanding of the lateral variations of velocity structure in the crust and upper mantle of the region expressing the continental collision between the Arabian and Eurasian plates. Our strategy is to combine different types of geophysical data sets, in this case, body wave travel time data and gravity data, in a formal joint inversion for velocity structure. Preliminary work has shown that body wave data and gravity data can be combined to yield improved resolution of the variability of crustal and upper mantle velocities. A key element to this success is careful filtering of the gravity data so that the signal source region corresponds to that which is sampled by the seismic data.

Our choice of region for this study is driven in part by the availability of an exceptional data set of body wave travel time data that results from a series of research projects on calibrated locations in the region. No other area of monitoring interest is so well sampled by ground truth events. This project is one effort to make maximum use of this unique data set.

RESEARCH ACCOMPLISHED

This is a new project and efforts so far have focused on assembling the computer codes and data sets.

Body Wave Data

The data set of body wave arrival times that will be used in this study will be derived from the catalog of earthquakes in the study region that has been steadily developed and groomed by Bergman in collaboration with E.R. Engdahl over the last 10 years (e.g., Bergman et al., 2009). The status of this catalog as of September 2009 is described here.

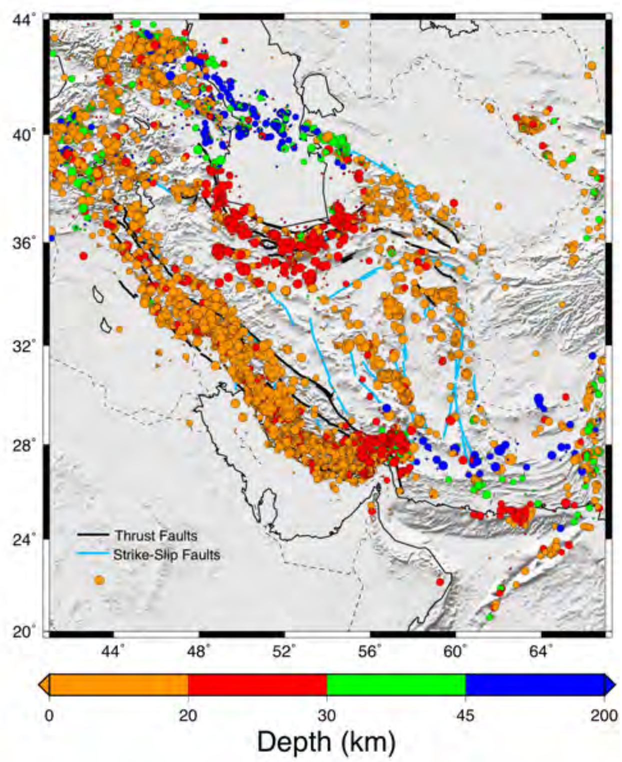

Figure 1. Events in our catalog that satisfy the condition of having secondary azimuth gap < 180°, calculated over the entire range of epicentral distances. Secondary azimuth gap is the largest azimuth gap that is filled by a single station. Focal depths are color-coded.

• The catalog contains 28,267 earthquakes in the study region, dating from 1923-2008. Most of the larger and better-recorded events have been reviewed by Engdahl (in single-event location mode, except for the most recent (post-2006) events, but new phase readings have been added to many of them.

- The catalog is substantially complete through 2006, the latest time for which we have ISC data. Data for events in 2007 and 2008 are mainly from the USGS Earthquake Data Reports (EDR) and local networks (through May 2008). Some data from local stations is reported by the EDR in the second half of 2008, when NEIC analysts have manually extracted the data from seismic network websites for events of interest.
- Depths: Where free depth solutions are not possible and there is insufficient depth phase data (or waveform studies) to constrain a fixed depth location, focal depths are set at regionalized default depths based on the analysis of Engdahl et al. (2006). Depths typically range from about 6-20 km.
- Magnitudes: Events with reported magnitude 2.5 or greater are retained for the catalog, but some events with declared magnitude less than 2.5 are included because they are well recorded. A number of events in the ISS period (1923-1963) have no reported magnitude but are known to be larger events. In the modern period, some events have no reported magnitude but have many phase readings and are probably larger than 2.5.
- 9657 events satisfy a criterion of having secondary azimuth gap < 180°. Events that don't meet this criterion have less accurate locations and are probably not suitable for tomography.

We will carry out the joint inversions using the data set of ~10,000 events which have a secondary azimuth gap of less than 180° (Figure 1). The locations and origin times of these events are not calibrated but their locations should have less bias than average and many of them have been reviewed. This would represent a data set that is fairly typical of those used in most tomographic studies. The density of raypath coverage for the phase Pn in an earlier version of the catalog is shown in Figure 2. Coverage in the southeastern portion of the region has been poor because of the scarcity of seismic stations in that area, as well as in neighboring countries. Several stations have been installed in the region in recent years and we hope for improvements in data coverage during the course of this project.

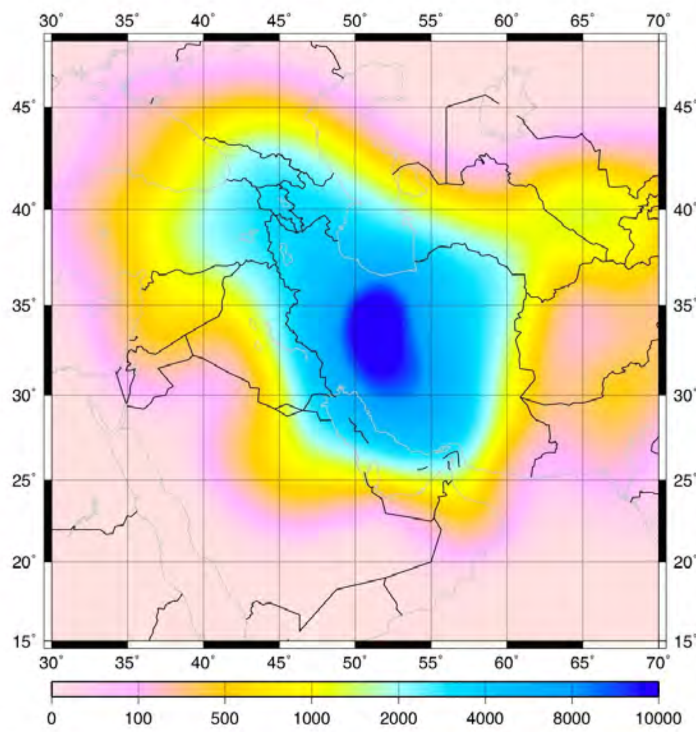

Figure 2. Ray density map for Pn in the study region, using an earlier version of the regional catalog.

We will also carry out joint inversions with a data set of much higher quality, consisting of the events that are members of calibrated earthquake clusters in the region (Figure 3).

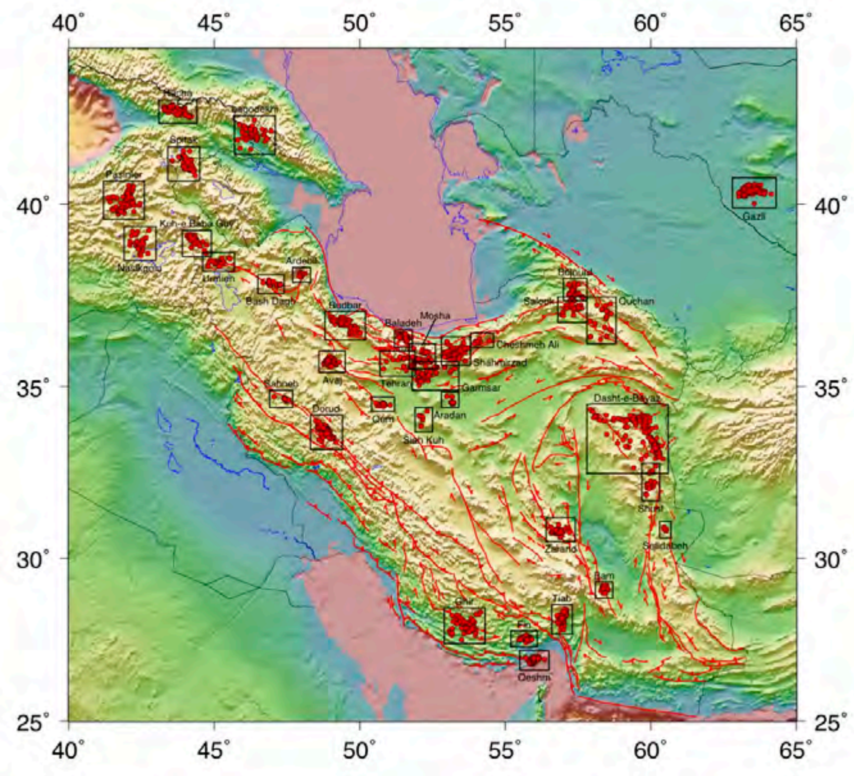

Figure 3. Location map of 35 clusters of earthquakes in the region that have been calibrated for absolute location and contain events that qualify as $GT5_{90}$ or better (~ 1700 events). Solid red circles are all earthquakes in a cluster, regardless of calibration level, but almost all events are $GT10_{90}$ or better.

The clusters contain 1834 events, of which 1699 qualify as $GT5_{90}$. Calibration is done through a multiple event relocation analysis and the use of near-source data of various types. Origin times are also calibrated, although they are coupled to focal depth, which is less well resolved than other source parameters. Through the calibration analysis, the arrival time data sets of these calibrated events undergo a rigorous and thorough grooming process that identifies outliers and leads to estimates of empirical reading error for most phase arrivals.

It is very unusual to have such a high quality data set that provides coverage over such a large region. Even so, the raypath coverage, especially for direct crustal phases (Pg, Sg), from the calibrated clusters leaves many parts of the region poorly-sampled or unsampled. We plan to carry out joint inversions in more limited regions in which coverage by the calibrated raypaths is adequate. These results can be compared to the results obtained from the larger, uncalibrated data set, to provide a validation process. Validation will also be performed by calculating residuals of the GT dataset through models derived from joint inversion of gravity and uncalibrated body wave data.

We will also explore the utility of performing multiple event relocation analysis on clusters of earthquakes, even when there is insufficient data to calibrate the location of the cluster. This is likely to improve resolution in the joint inversion analysis in several ways:

• Relative locations of all events in a cluster will be significantly improved.

• Events with poorly-constrained locations (even though they may pass the requirement for secondary azimuth gap) can be identified and removed from the data set.

• The relocation analysis is very effective at identifying outlier readings, which can be flagged and removed from the data set for inversion.

There will still be unknown bias in the location of the cluster, but the bias will be identical for all events in the cluster. Therefore the traditional “event” terms in tomography can be replaced by a much smaller number of “cluster” terms.

Even with these efforts to provide raypath coverage with well-constrained sources, there will be regions that have little or no coverage for crustal phases, thus limiting what can be gained from the joint inversion concerning crustal velocity structure. It is our expectation that supplementing the body waveform data with gravity data will provide additional resolution in these regions.

An Example: Avaj

To illustrate the application of our multiple event relocation methodology for calibrated locations we present more detailed information about one calibrated cluster, Avaj (see Figure 3 for location). This cluster was based on a large (M_W 6.4), damaging earthquake on June 22, 2002 and it's aftershocks. The cluster of 89 events includes 5 events prior to the mainshock and aftershocks as recent as March 2008. In early studies of this cluster (Walker et al., 2005) we used indirect calibration with one of the aftershocks that was reasonably well located by a temporary deployment of seismometers, but this event was not very well linked to the rest of the cluster by readings at common stations and the calibration was not very robust. More recently we obtained readings from the aftershock survey for other events and more importantly, readings from more recent events recorded at new permanent seismic stations that provided enough azimuthal coverage at local distances to permit a very robust calibration using the direct method (Figure 4). 88 events in the cluster qualify as $GT5_{90}$ or better.

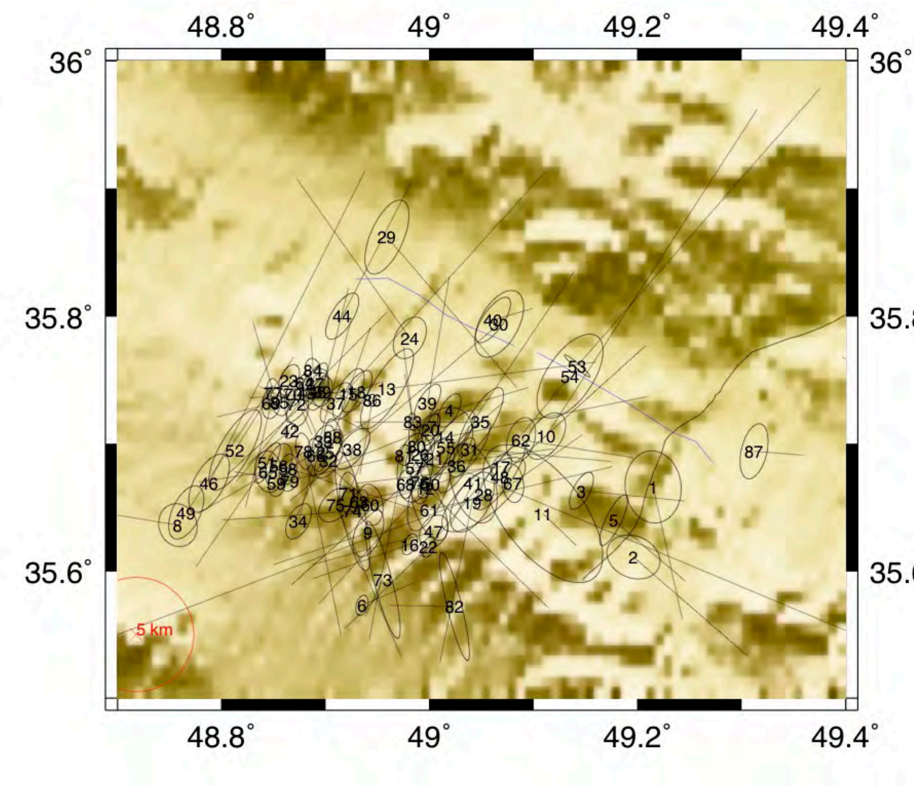

Figure 4. Calibrated locations for the Avaj cluster. Confidence ellipses are shown for absolute location at 90% confidence level. Vectors show the change in location from starting locations (single event catalog locations). A circle of 5 km radius shown for reference.

The calibration was done with direct P and S readings out to a distance 1.7°, using a single layer crustal model that was adjusted in thickness and velocity to match the slopes of the main phases and the Pg-Pn crossover distance (Figure 5). It is evident that correct phase identification becomes problematic beyond the cross-over distance. We investigate the local distance readings carefully for every cluster that will be calibrated using the direct method, to ensure that the assumed velocity model adequately accounts for the arrival time data and phase identifications, and also to determine where the assumption of a 1-D model begins to break down. When there is data at very short range, such as the S-P readings in Figure 5, the degree of flattening of the observed travel times provides strong constraint on focal depth. In this case there is little flattening because the earthquakes are quite shallow. An average assumed depth of 8 km fits the data well.

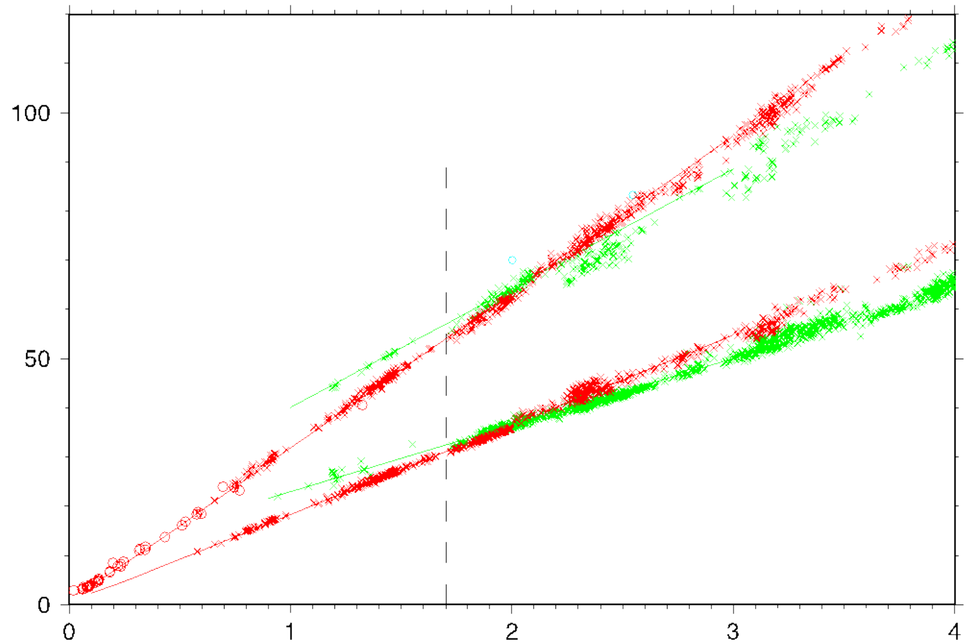

Figure 5. Travel-time vs. distance plot for local distances for the Avaj cluster. Pg and Sg are shown as red X's. Pn and Sn arrivals are shown in green. Theoretical travel times from the assumed single layer crustal model are shown. Circles are other phases. In particular the ones at distances less than 0.8° are S-P times from nearby accelerometer stations with uncalibrated timing. The S-P times have been added to the corresponding theoretical P time for proper comparison with the theoretical S arrival time.

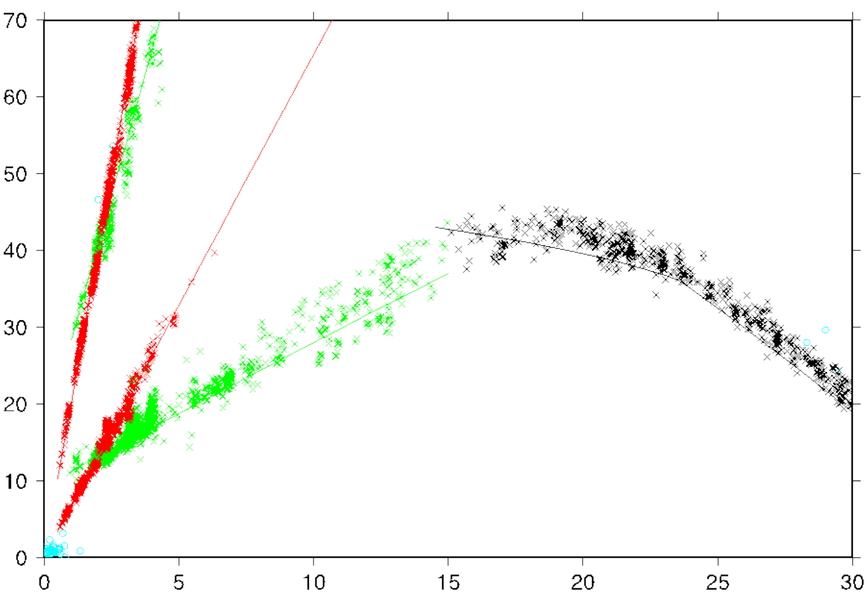

Figure 6. Travel-time vs. distance plot for regional distances for the Avaj cluster. Pg and Sg in red, Pn and Sn in green, P in black. Theoretical travel times at less than 15° are from a single layer crustal model with crustal thickness (47 km) adjusted to fit the Pn data. Teleseismic travel times are from ak135.

The variability in arrival times of Pn are shown in Figure 6. The variability would be even greater with the original data set. This data set has been carefully edited for outlier readings, based on the consistency of multiple observations of the same phase at the same station. It is this variability that we are primarily interested in explaining with a 3-D model determined in the joint inversion (with gravity data) described below.

Note that when the origin times are established by near-source data, the theoretical travel times for teleseismic P are too early by several seconds. This is mainly because ak135 assumed a crustal thickness of 35 km. Crustal thickness in the study region ranges from 45-60 km. Therefore, travel times are increased by the extra path length in the crust. This result has been observed with virtually every calibrated cluster in the region, and is one of the reasons that teleseismic locations have systematic bias.

Gravity Data

Gravity data will be extracted from the global gravity model derived from the Gravity Recovery and Climate Experiment (GRACE) satellite mission. A detailed description of the satellite data and the computation of the gravity field are given by Tapley et al. (2005). The new gravity field is more accurate than previous data and reveals previously unobservable tectonic features. Figure 7 shows the free-air gravity anomalies for the proposed study region. Blue colors represent gravity highs and gravity lows are represented in red.

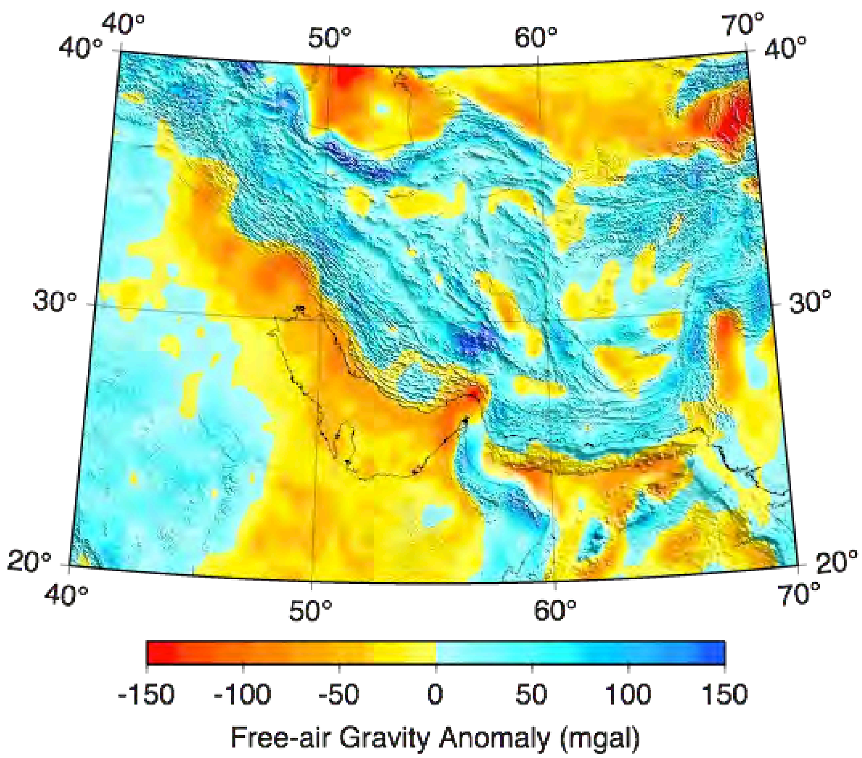

Figure 7: Free-air gravity observations for the proposed region of study. These anomalies have been extracted from the global gravity model derived from the GRACE satellite mission. Red colors represent gravity lows, blue colors indicate gravity highs. Data are available at http://www.csr.utexas.edu/grace/gravity, last accessed June, 2010.

Free-air gravity anomalies contain information not only of the subsurface density but also topography. While in flat regions this may not be a problem, in areas of high topographic relief this effect needs to be removed; thus, free-air anomalies will be converted into Bouguer anomalies assuming a standard density for crustal rocks of 2670 kg/m^3.

Modrak et al. (2010) have shown that filtering the gravity data provides important balance such that crustal density variations of higher spatial frequency can be exploited for imaging shallow structure, whereas mantle contributions

can be assumed to produce the longer-period gravity signals. Judicious application of filtering is an important aspect of our analysis so that contributions from crust and mantle are handled appropriately, and we will employ the methods of Modrak et al. (2010) with attention to selecting the optimal spectral band to employ in our joint inversion.

Joint Inversion of Body Wave and Gravity Data

The results of Maceira and Ammon (2009) demonstrated that joint inversion of surface wave and gravity data offers a simple and elegant compromise between fitting both data sets and improves the V_S model. In turn, this will enhance earthquake location and characterization. In this project we explore the power of a similar joint inversion method, combining seismic body wave travel times and Bouguer gravity anomalies.

Our joint inversion of seismic body wave travel times (P and S) and Bouguer gravity anomalies will be undertaken using a new code adapted from Maceira and Ammon (2009) and integrated into the regional version of *TomoDD* (Zhang and Thurber, 2003).

Our treatment of the gravity data is similar to that of Maceira and Ammon (2009). The gravity anomaly Dg at a point (x, y, z) is due to density anomalies Dr) in a volume. We follow Plouff (1976) to calculate the 3-D gravity anomalies of a prism with arbitrary dimensions (Figure 8).

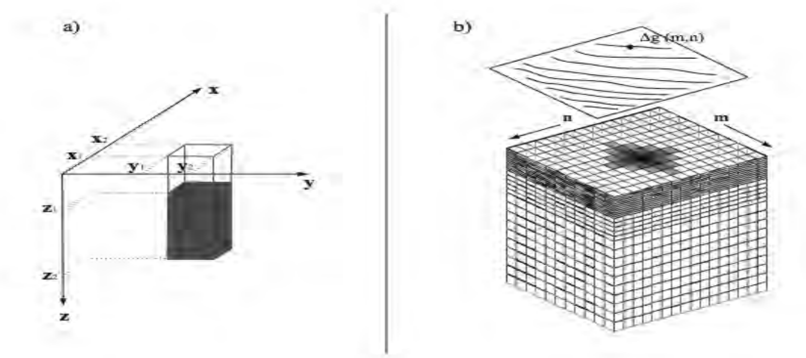

Figure 8: Gravity anomaly calculation for a 3D model. (a) The gravity anomaly associated with a rectangular prism of constant density can be computed analytically following Plouff (1976). (b) The gravity anomaly at a given observation point Δg(m, n) (black square) can be computed by adding the contribution of all the resultant gravity anomalies of all prisms in the shaded area of the model.

In Maceira and Ammon (2009) the prisms used in the computation of the gravity anomalies coincide with the cells in the gridded model. Therefore each cell in the model is a column of prisms with horizontal dimensions of 1º by 1º and the corresponding layer thickness value as the third dimension. The contribution of each cell to the gravity value at a given point is a decaying function of the distance. Beyond a certain distance, the effect is negligible. Therefore, the sensitivity of gravity anomaly to the density (or, through scaling, to seismic velocity) is only calculated for cells within a prescribed distance. The sensitivities of gravity to density in each cell are calculated by perturbing its value by 5% while keeping the values of other cells fixed.

We have modified this approach by attaching the density values, calculated previously in each 1x1 degree column of blocks, to the nodes that are being modeled on the 3D grid. This augments the matrix we invert for our updated model, and increases the size of the problem accordingly. Solving for the full three-dimensional system has required the adoption of an LSQR approach, rather than the SVD used in Maceira and Ammon's one-cell-at-a-time approach.

Density - Velocity Relations

One of the difficulties with joint inversions is to determine a relationship between the independent data sets. In this case, we require constraints between seismic velocities and density. There is not a unique and universal relationship applicable to all types of lithologies at every single depth under all possible conditions of temperature and pressure. LANL is currently testing, in collaboration with M.I.T., three different relationships between seismic velocities and density: (1) a combination of two existing empirical relationships; one more suitable for sedimentary rocks after Nafe and Drake (1963) and the well-known Birch's (1961) law more appropriate for basement rock; (2) Brocher's

(2005); and (3) Harkrider's (personal communication). An advantage of the Harkrider relationship is that it allows independent estimates of Vp and Vs as functions of density, thus eliminating the requirement of making an *a priori* assumption of a fixed Poisson ratio. The new code, JointTomoDD, is currently being tested at LANL as well as at the Massachusetts Institute of Technology (MIT), for a variety of tectonic settings such as the Tarim Basin, China, the crust and subduction zone beneath western Colombia, and a thermally active region within Utah in the central United States.

Preliminary tests of the body-wave and gravity joint inversion suggest that a key influence on the successful modeling is that of relative weighting of the two datasets. Our work in this project will emphasize detailed characterization of the tradeoffs between these parameters and a careful comparison of the obtained models with known features in the study area, although the ultimate validation will be testing the travel-time predictions of the final models for known GT paths.

CONCLUSIONS AND RECOMMENDATIONS

Because this project is just starting it is premature to formulate conclusions or make recommendations.

REFERENCES

Bergman, E. A., E. R. Engdahl, M. H. Ritzwoller, and S. C. Myers (2009). Crustal structure from in-country and ground-truth data, in *Proceedings of the 2009 Monitoring Research Review: Ground-Based Nuclear Explosion Monitoring Technologies*, LA-UR-09-05276, Vol. 1, pp. 22–31.

Birch, F. (1961). The velocity of compressional waves in rocks to 10 kilobars, part 2, *J. Geophys. Res*., 66: 2199– 2224.

Engdahl, E. R., J.A. Jackson, , S. C. Myers, E. A. Bergman, and K. Priestley (2006). Relocation and assessment of seismicity in the Iran region, *Geophys. J. Int.*, 167: 761–778.

Maceira, M. and C. J. Ammon (2009). Joint inversion of surface wave velocity and gravity observations and its application to Central Asian basins shear velocity structure, *J. Geophys. Res*., 114, B02314, doi:10.1029/2007JB005157.

Modrak, R. T., M. Maceira, J. Van Wijk, and M.E. Pasyanos (2010). Rift structure of East Africa from joint inversion of group velocity estimates and gravity data. GRL pp. 1–12.

Plouff, D. (1976). Gravity and magnetic fields of polygonal prisms and application to magnetic terrain corrections, Geophysics, 41: 727–741.

Nafe, J. E. and C. L. Drake (1963). Physical properties of marine sediments, in *The Sea*, vol. 3, edited by M. N. Hill, pp. 794–815, Interscience, New York.

Tapley, B.D., S. Bettadpur, J.C. Ries, P.F. Thompson, M.M. Watkins (2005), GRACE measurements of mass variability in the Earth system, *Science*, 305: 503–505.

Walker, R. T., E. Bergman, J. Jackson, M. Ghorashi, and M. Talebian (2005) The 2002 June 22 Changureh (Avaj) earthquake in Qazvin province, northwest Iran: epicentral relocation, source parameters, surface deformation and geomorphology, *Geophys. J. Int.*, 160: 707–720.

Zhang, H., Maceira, M., Toksoz, M., Burlacu, R., Rowe, C., and Y. Yang (2009). Joint geophysical imaging of the geothermal sites in the Utah area using seismic body waves, surface waves and gravity data, Amer. Geophys. U. Fall Meeting.

DISTRIBUTION LIST

DTIC/OCP 8725 John J. Kingman Rd, Suite 0944 Ft Belvoir, VA 22060-6218	1 cy
AFRL/RVIL Kirtland AFB, NM 87117-5776	2 cys
Official Record Copy AFRL/RVBYE/Robert Raistrick	1 cy